Solar thermal, rear-ventilated façades as heat pump sources in multi-storey buildings

Edward Frick[1], Christoph Büttner[1], Maik Kirchner[1]and Federico Giovannetti[1]

[1] Institute for Solar Energy Research in Hamelin (ISFH), Emmerthal, Germany

Abstract

The envelope of multi-storey residential buildings offers an untapped potential for the integration of renewable energy supply systems. Due to their specific assembly, rear-ventilated façades exhibit particularly suitable features in this regard: high design flexibility, modularity, easy installation and maintenance as well as the possibility to hide the systems engineering in the ventilation gap. We analyze solar thermally activated façade claddings made of glass, concrete and metal by means of laboratory tests on single façade modules as well as in-situ experimental tests on large-sized façade prototypes, focusing on thermal performance and reliability. We report very different characteristic values, depending on the specific cladding design and on the approach used for the activation: In case of the metal-façade, the zero-loss efficiency η_0 ranges from 0.39 to 0.71 and the heat-loss-coefficient ranges from 6.65 to 14.55 W m^{-2} K^{-1} under laboratory conditions. For the large-scale outdoor façade we determined a zero-loss efficiency of 0.6 and heat-loss-coefficient of 11.24. Based on these results, the potential of the façades as sources for ground-coupled heat pumps is assessed by building simulations with the software TRNSYS for different configurations of the heat supply system. The solar façade reduces the load on the borehole heat exchangers up to 50% and enables a smaller dimensioning of the field.

Keywords: Rear-ventilated façades, solar thermal collectors, TRNSYS, multifamily buildings, heat pump, building envelop, thermal activation, building integration

1. Introduction

In order to reduce carbon-dioxide emissions and achieve a climate neutral energy and heat supply in the building sector, a much greater use of renewable energies as well as the development and the implementation of novel concepts for renewable heat generation in multi-storey buildings are required. For this purpose, European and national directives are tightening the requirements for existing and new buildings focusing on higher renovation rates and on a more effective substitution of fossil fuels. Solar thermal energy and heat pumps can significantly contribute to the heat supply of buildings. While both technologies are becoming more and more common in single-family houses, the technical implementation in multi-storey residential buildings is difficult due to the limited space available both for collectors and heat pump sources.

The integration of solar thermal components in the building envelope offers untapped potential for new solutions with high architectural quality. Rear-ventilated façades are particularly suitable for the solar-thermal activation due to various reasons: The modular design of rear-ventilated façades enables prefabrication and an uncomplicated installation of the activated façade elements. Furthermore, the rear-ventilation gap offers the possibility to hide the systems components (tubing, heat exchangers, etc.). Finally, the wide range of available cladding materials allows the realization of different solutions with a high design flexibility.

A stated goal of the project is to support or replace conventional heat pump sources and thus accelerate the energy-oriented refurbishment of urban areas. Conventional heat sources like borehole or air heat exchangers do need appropriate space outside the building. These additional heat sources can be reduced or replaced, if building envelopes can actively contribute to the energy production.

doi:10.18086/swc.2021.43.01 Available at http://proceedings.ises.org

2. Façade concepts

The basic assembly of a rear-ventilated façade as shown in Fig. 1 consist of the external wall, the façade cladding and a substructure, which builds the static link between the wall and the cladding elements. The substructure is usually built up by wall brackets, which are attached to the anchoring base with a thermal separation, as well as vertically or horizontally running supporting profiles, which hold the façade claddings via visible or hidden fastening elements (FVHF, 2018). The separation between the cladding and the building insulation creates a ventilation gap, which has positive effects on the building's humidity and indoor climate and is the essential characteristic of a rear-ventilated façade. Solar irradiation on the cladding elements creates a natural convection inside the ventilation gap, which drains moisture from the building's insulation. To ensure a sufficient air flow, the depth of the rear-ventilation gap is required to be at least 20 mm with inlet and outlet openings with a cross-section of at least 50 cm² per meter wall length (DIN, 2010).

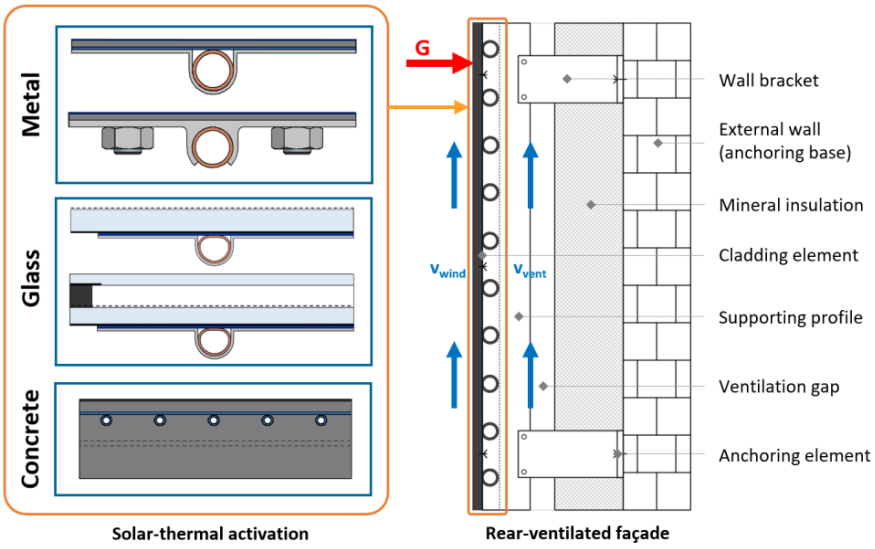

Fig. 1: Left: Investigated concepts for the solar-thermal activation of rear-ventilated façades. The thermal activation is achieved by implementing different types of heat-exchangers to façade claddings out of concrete, glass and metal. Right: Basic scheme of a rear-ventilated façade

The main development approach for the solar-thermal activation in this project is to apply heat-exchangers to the façade cladding elements and utilize them as solar-absorbers, without modifying the existing façade systems, so that the original appearance of the non-activated façade remains unchanged. For this purpose, we study three different façade systems with cladding elements made of concrete, glass and metal. A main challenge in this regard is to ensure a durable connection with a good thermal contact between cladding elements and heat-exchangers. Fig. 1 shows the concept for the solar-thermal activation for each material.

The development of the solar-thermal activated glass-façade is based on the results of previous research work at the ISFH (Kirchner et al., 2017). Two different types of glasses are analyzed as cladding elements as shown in Fig. 1: Single glazed enameled glass panels and enameled insulation glasses. In both cases the solar irradiation is absorbed in the enamel layer and converted into heat. The generated heat is transferred to the fluid by means of heat-exchangers placed on the rear side of the glass. The heat-exchangers consist of a D-shaped copper tubing and are applied to the glass with heat conducting plates and an adhesive bonding (SolMetall, 2017). The D-shape of the tubing allows heat conduction over a large part of the tubing surface. The heat losses due to long wave irradiation can be reduced by means of a low-emitting layer on the front side of the glass. In case of the insulation glasses the heat-losses are further reduced by introducing an additional front pane separated from the absorber glass panel with a hermetically sealed air or inert gas gap. That way it is possible to generate heat at higher temperatures and, for example, enable direct solar domestic water heating.

For the solar-thermal active metal façade, we investigate cladding elements out of aluminum due to its high thermal conductivity. The connection between heat exchangers and cladding elements is in this case realized either by means of an adhesive bonding or by a form-fitting connection with welded threaded bolts and nuts. In addition to the concept used for the glass façade, we analyze a geometry, with the copper tubing attached to clamp-profiles

as shown in Fig. 1. This method is commonly used by the façade manufacturers involved in the project for the connection of the cladding elements to the substructure. By applying the same fixing approach for the heat-exchanger as well, process steps during the production and correspondent costs can be reduced. Furthermore, a higher sustainability as well as an easier building approval procedure can be achieved by avoiding the use of an adhesive bonding for the building envelope. By combining the form-fitting connection with clamp-profiles as heat exchangers we expect a better thermal connection than with heat-conducting plates due to the higher thickness of the clamp profiles.

For the thermal activation of the concrete façade so-called capillary tube mats made of polypropylene (PP-R) are embedded directly into the concrete slab. The capillary tube mats consist of a series of plastic tubes with an inner diameter of 2.7 mm placed at a distance of 20 mm to each other. The tubes are connected with manifolds with an inner diameter of 20 mm, creating a parallel connection of the capillary tubes. The impact on the thermal efficiency of the position of the capillary tube mat inside the concrete slab as well as different coatings are analyzed in the project. Another investigation topic is the effect of the activation and of the correspondent operation conditions on the hygrothermal behavior of the concrete cladding.

3. Laboratory tests

For the analysis and optimization of the thermal efficiency of the solar-thermal active metal façade various laboratory tests on different prototypes have been carried out. In the first step we characterized the optical properties of different surface coatings by measuring the reflectance from the ultraviolet to the infrared-range of the electromagnetic spectrum (250 nm to 17 µm wavelength) on small-scaled cladding samples by using two different spectrometers both equipped with integrating spheres (Cary 5000 from Varian/Agilent Technologies® and FTIR Equinox from Bruker®). Tab. 1 shows the determined solar absorptance and thermal emittance for a selection of common surface coatings, calculated according to ISO 9050 (absorptance) and Planck's radiation law (thermal emittance) at a temperature of 373 K.

Tab. 1: Determined solar absorptance and thermal emittance of common surface coatings for metal-façade claddings

Colour	**RAL-tone**	**Solar absorptance** (±0.01)	**Thermal emittance** (±0.02)
Jet black	RAL 9005	0.95	0.94
Graphite black	RAL 9011	0.95	0.95
Clay brown	RAL 8003	0.82	0.92
Iron grey	RAL 7011	0.89	0.96
Anthracite grey	**RAL 7016**	**0.92**	**0.96**
Silver grey	RAL 7001	0.72	0.94
Blue grey	RAL 7031	0.86	0.95
Emerald green	RAL 6001	0.76	0.93
Gentian blue	RAL 5010	0.75	0.90
Brilliant blue	RAL 5007	0.81	0.94
Red orange	RAL 2001	0.57	0.93
Flame red	RAL 3000	0.63	0.92
Ruby red	RAL 3003	0.66	0.92
White aluminium	RAL 9006	0.58	0.90
Pearl dark grey	RAL 9023	0.81	0.94
Cream	RAL 9001	0.27	0.92
Light ivory	RAL 1015	0.35	0.92

For the analysis of the thermal efficiency of the activated metal façades several prototypes with a cladding element size of 2250x1166 mm^2 have been manufactured. For the surface coating we chose the RAL-tone 7016 with a solar absorptance of 0.92 and thermal emittance of 0.96. The prototypes differ in the geometry of the heat-exchanger (Type 1: heat-conducting plates, Type 2: clamp-profiles) and the fixing method to the cladding element as described in section 2. Furthermore we varied the number of tubes and the distance between the pipes (80 mm, 100 mm and 150 mm) of the heat exchanger. At last, we also modified the number of threaded bolts, to study the impact on the heat conduction of the contacted area.

The collector efficiency measurements have been carried out in a sun simulator according to the standard testing procedure (DIN EN, 2018) and the correspondent efficiency coefficients for uncovered assembly based on eq. 1 have been determined. The tests have been performed both with a closed and an opened rear-ventilation gap (depth of the gap: 45 mm), so that a higher air flow on the rear side of the modules due to the artificial ventilation is achieved in the latter case. Tab. 2 shows the results of the performance measurements.

$$\eta = \eta_0 \cdot (1 - b_u \cdot v) - (b_1 + b_2 \cdot v) \cdot \frac{\Delta T}{E_n} \qquad \text{(eq. 1)}$$

Tab. 2: Results of the efficiency measurements for prototypes of solar-thermal active metal-façade claddings.

Module variant	Ventilation gap	η_0 [-]	b_1 [W m^{-2} K^{-1}]	b_2 [J m^{-3} K^{-1}]	b_U [s m^{-1}]
Type 1, adhesive bonding, 80 mm pipe-distance	Open	0.70	14.55	2.80	0.075
	Closed	0.71	12.88	1.75	0.061
Type 1, adhesive bonding, 100 mm pipe-distance	Open	0,67	13,95	2,7	0,077
	Closed	0,67	11,41	1,48	0,057
Type 1, adhesive bonding, 150 mm pipe distance	Open	0,58	11,25	1,86	0,096
	Closed	0,59	9,90	1,12	0,072
Type 1, form-fitting bonding, 80 mm pipe distance	Open	0.54	11.66	1.91	0.101
	Closed	0.54	9.44	0.92	0.079
Type 1, form-fitting bonding, 100 mm pipe distance	Open	0,49	10,27	2,17	0,086
	Closed	0,50	8,89	1,64	0,071
Type 1, form-fitting bonding, 150 mm pipe distance	Open	0,41	8,47	1,18	0,120
	Closed	0,39	6,65	0,62	0,091
Type 2, form-fitting bonding, 100 mm pipe distance	Open	0,58	11,74	1,66	0,109
	Closed	0,56	9,86	1,22	0,069
Type 2, form-fitting bonding, 100 mm pipe distance, increased bolt number	Open	-	-	-	-
	Closed	0.59	10.39	1.04	0.082
Type 2, form-fitting bonding, 100 mm pipe distance, reduced bolt number	Open	0.54	11.70	1.66	0.111
	Closed	0.54	10.17	0.99	0.044

As expected, the module with heat-conducting plates and an adhesive bonding report the highest performance with zero-loss collector efficiencies varying from 71% to 58%, depending on the pipe-distance. On the contrary, the zero-loss efficiency of the variant with heat-conducting plates and a form-fitting connection reaches a maximum of 54% for the module with a pipe-distance of 80 mm and about 50% with a pipe-distance of 100 mm. Comparing the results of the different examined heat exchanger geometries, the variant with clamp profiles reaches higher efficiencies than the variant with heat conducting plates anda form-fitting connection, due to the more homogenous contacted area to the cladding elements. The basic design with 80 threaded bolts per module

reaches a zero-loss efficiency about 56% with a closed ventilation gap. The variation of the bolt number showed little impact on the performance results: Increasing the bolts to 110 units per module improved the zero-loss efficiency to about 59%, while reducing the bolts to 40 units per module reduced it to 54%. The heat loss coefficients showed values comparable to standard uncovered collectors ranging from 6.65 to 14.55 W m^{-2} K^{-1}.

4. Outdoor tests

On the basis of the laboratory tests on the activated metal claddings a module design was selected and a large-scale thermally activated metal façade was installed on an outdoor test wall, to study the thermal behavior of the façade under real weather conditions. Fig. 2 shows a schematic of the components of the test wall.

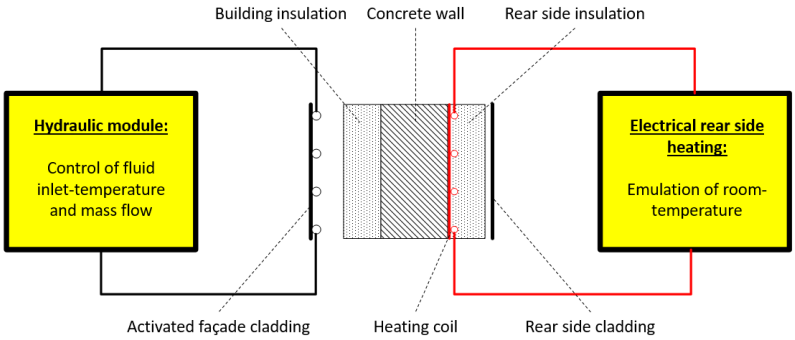

Fig. 2: Schematic of the outdoor test wall components. Inlet-temperature and fluid mass-flow are controlled by a hydraulic unit. The room-temperature is emulated via an electrical rear side heating.

The test wall features hydraulic modules for two separate fluid-circuits, enabling the parallel operation of two activated façades. The hydraulic modules allow an operation of the façades with controlled inlet temperatures down to -15 °C and controlled mass flow up to 1600 kg h^{-1}. The controlled fluid temperature is provided by a cooling unit consisting of a water chiller and a 1000 l fluid tank. To emulate the room temperature on the interior side of the wall, surface heating panels have been mounted to the wall's rear side. The heating panels consist of aluminum sheets with attached wires. By controlling the electrical power through the heating wire, a homogenous temperature of about 19 °C on the wall's rear side can be achieved. To reduce temperature fluctuations and heat losses to the environment an additional insulation (16 cm) has been installed on the aluminum sheet.

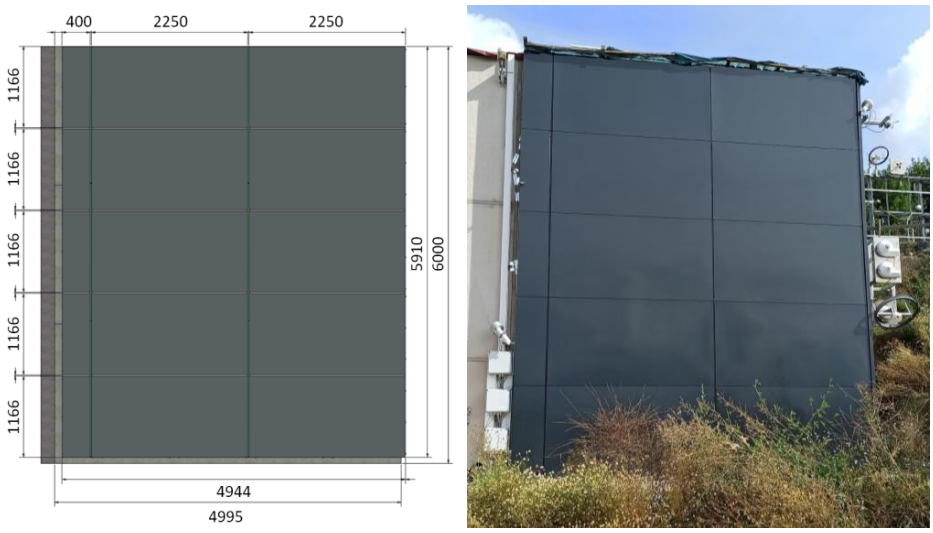

Fig. 3: Left: Layout of the large-scale solar-thermal activated metal façade. Right: Metal-test façade on the outdoor test wall

The installed metal façade features ten identical active cladding elements each with an area of 2250x1166 mm² and an anthracite grey surface coating (RAL-tone 7016, $\alpha = 0.92$, $\varepsilon = 0.96$). The total area of the activated façade amounts to 26.23 m². The façade was installed with a distance of 60 mm between cladding and insulation (mineral wool, thickness: 18 cm, thermal conductivity: 0.035 W m^{-1} K^{-1}). For the solar-thermal activation we chose the

heat exchanger concept with clamp-profiles, a pipe-distance of 100 mm and a form-fitting connection with 80 threaded bolts per module as described in chapter 2 and examined in chapter 3. The hydraulic connection of the active façade elements to the fluid circuit is achieved by means of four manifolds placed in the middle of the façade, so that a parallel flow through all elements is realized. The connection to the manifolds is achieved by using flexible tubes with hydraulic plug-in connectors. In addition to the active elements a small area (2.33 m²) with standard, non-active cladding elements has been installed as reference. The complete layout of the installed metal façade is shown in Fig. 3.

The investigations on the large-scale active metal façade requires the measurement of various physical values. Fig. 4 gives an overview of the installed measurement equipment. For the analysis of the solar-thermal efficiency various meteorological data are recorded, including several radiation quantities in the façade plane like the hemispherical solar irradiance via a pyranometer, the longwave irradiance via a pyrgeometer and the diffuse irradiance via a pyranometer with shadow ring. Other measured quantities are the wind speed in the façade plane, the relative humidity and the temperature of the ambient air. To investigate the thermal behavior inside the rear-ventilation gap additional sensors were installed: several PT-100 temperature sensors to record the surface temperature on the cladding elements, two flow sensors to measure the velocity of the air flow, two combined sensors for the measurement of the air humidity and temperature and two special CHM-sensors developed at the Fraunhofer-Institute for Building Physics to directly determine the heat-transfer coefficient on the cladding element (Mayer et al., 2018). By measuring the heat-transfer coefficient, the air temperature and the surface temperature of the cladding element, the heat flow from the ventilation gap to the façade and vice versa can be determined. Furthermore, a heat flow plate was installed on the wall to analyze the impact of the solar-thermal activation on the heat transfer mechanisms through the wall.

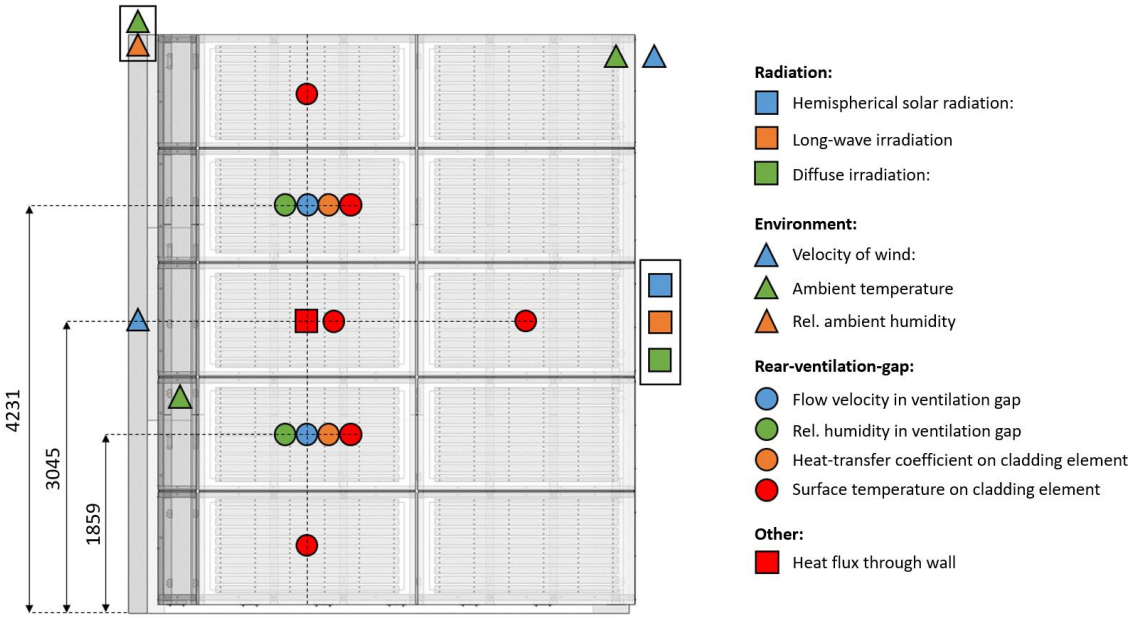

Fig. 4: Schematic of the measured physical values on the large-scale solar-thermal activated metal façade

In the first step a stationary performance evaluation of the active façade based on the test procedure described in (DIN EN, 2018) was carried out. For the tests the façade was operated with a fluid mass flow rate of 1600 kg h^{-1} to ensure turbulent flow during the entire testing period. The fluid inlet temperature was frequently varied over the period of several weeks to record data with a high variety of temperature differences. The resulting collector efficiency coefficients for uncovered collectors based on eq. 1 are shown in Tab. 3. Fig. 5 shows a comparison between the efficiency curves determined by means of the laboratory tests and the test under real weather conditions at an irradiance of 800 W m^{-2} and wind speed of 0.3 m s^{-1}. With a zero-loss efficiency of about 60% the large-scale activated façade reaches slightly higher performance values than the single module under laboratory conditions, both with an open and closed ventilation gap. The thermal performance at higher temperatures are comparable to the results of the single module measurement with a closed ventilation gap, due to the low flow-rates on the rear side of the large-scale façade modules compared to the flow rates during the

laboratory measurement with an open ventilation gap. The wind-dependency of the heat loss coefficient b_2 and of the zero-loss efficiency b_U are significantly lower for the large-scale façade than the laboratory results in both cases. The deviations result from the low variation in wind speed and generally low wind velocities recorded during the measurement period of the outdoor façade as well as from the different turbulence conditions occurring in the laboratory tests.

Tab. 3: Comparison between determined collector efficiency coefficients for indoor and outdoor measurements

Testing conditions	η_0 [-]	b_1 [W m^{-2} K^{-1}]	b_2 [J m^{-3} K^{-1}]	b_U [s m^{-1}]
Outdoor	0.60	11.24	0.84	0.024
Sun-simulator, open ventilation gap	0,58	11,74	1,66	0,109
Sun-simulator, closed ventilation gap	0,56	9,86	1,22	0,069

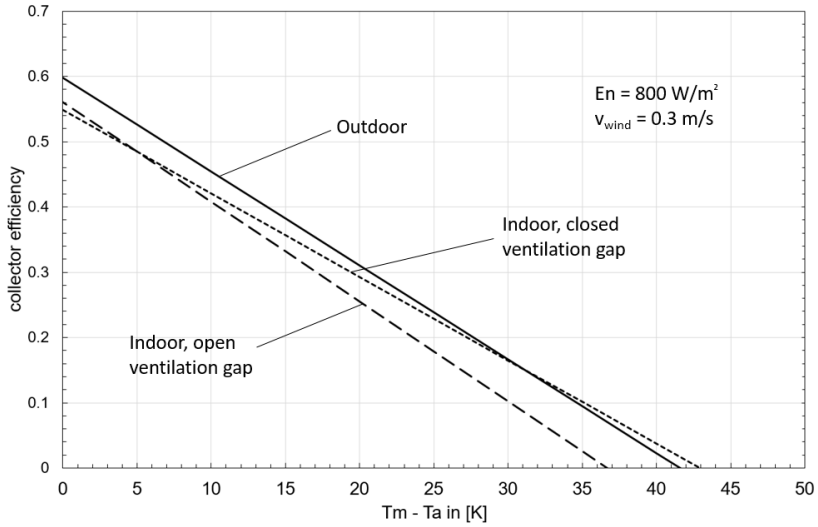

Fig. 5: Comparison between collector efficiency curves of the active metal façade determined by means of the laboratory tests and under real weather conditions for a wind speed of 0.3 m s^{-1}

5. System Simulation

To evaluate the behavior of the different façade concepts described in section 2 within a heat supply system, TRNSYS-simulations (Klein, 2014) of a multi-storey building were used.

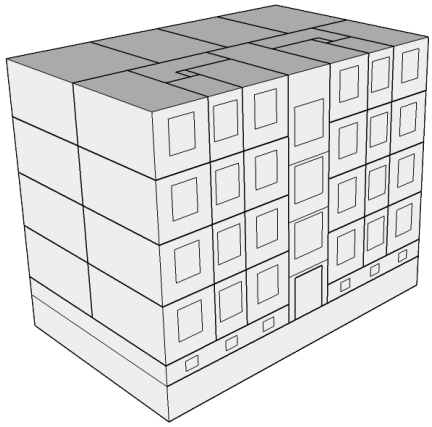

Fig. 6: Multi-storey residential building featuring 8 flats on 4 floors each with 84 m² living space

The freestanding building consist of 4 floors, each of them featuring 2 flats with 84 m² living space. The south and north façade are equipped with windows Fig. 6. The structural and heating system are chosen according to the current standards for buildings, the boundary conditions assumed for the simulation are stated in Tab. 4.

Tab. 4: Boundary parameters used for the TRNSYS-simulation

Weather data	DWD weather data (BBSR, 2017), mean year of present-day test reference year based on the measurement and observation data 1995 to 2012 („TRY2015 Jahr“) for coordinates 48.8975°, 08.7083° (Pforzheim, Germany)
Building	Freestanding multi-storey building with basement, orientation south with a deviation of 13° to east, 672 m² living space, usable area of 1024 m², Type 56
Heat demand / useful heat	34,170 kWh (space heating and tap water)
Demand space heating	23,110 kWh (34.4 kWh/m²), floor heating Type 362 (S. Holst, 2010)
Demand hot tap water	11,060 kWh (70 - 112 l/d per flat, 45 °C set temperature)(Braas et al., 2020)
Heat generation	37,400 kWh (heat loss buffer storage 1700 kWh)
Buffer storage	1,000 l, 1.8 m high, heat loss 5 W/K
Thermally activated façades	Different cladding materials (concrete, metal, glass) and different areas
Heat pump	Modulating brine-water heat pump; Performance values: COP B0/W35: 4.7 (35%) 4.17 (65%) 3.9 (75%) COP B5/W35: 5.4 (35%) 4.6 (65%) 4.3 (75%); sources: solar façade and borehole heat exchanger; sinks: buffer storage stratified loading of two sections,
Borehole heat exchanger (BHE)	Field of 3 probes with a length of 75 m and a spacing of 6 m

The difference between generated and useful heat originates from the heat losses of buffer storage, riser pipes and decentral instantaneous water heater (IWH). These losses are internal building gains. The simulation is carried out with weather data from Germany's National Meteorological Service, the Deutscher Wetterdienst (DWD) (BBSR, 2017).

The system consists of thermally activated façades, a brine-water-heat pump, borehole heat exchanger, a hydraulic switch, a buffer storage, riser pipes, a decentral instantaneous water heater in each flat, a floor heating system (flow and return temperature 35/32 °C) and single-room air handling unit with heat recovery in each room except corridor, and external shading devices on all windows. The system configurations can be related to the generic system classifications shown in Fig. 7 equivalent to the representation of the energy flows of IEA SHC Task 44 (Frank et al., 2010).

The thermally activated façade serves both as a solar collector and environmental heat exchanger. It not only enables the regeneration of the ground but can also be used as a direct source for the heat pump. Additionally to the borehole heat exchangers, the heat pump loads a buffer tank (Fig. 7). Because of different mass flow occurring in façade, borehole heat exchanger and evaporator of the heat pump, a hydraulic switch is used to connect the three units.

This centralized storage enables the use of decentral instantaneous water heater (IWH) in each flat for domestic hot water heating as required. The floor heating system is controlled to keep the set temperature. Because of the IWH the supply temperature is set all year to 35 °C. A schematic of the system is shown in Fig. 8.

Shading device and air handling unit are used as overheating and glare protection.

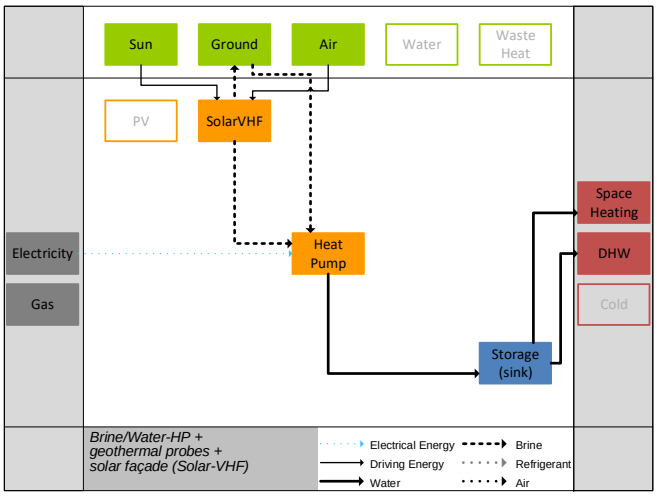

Fig. 7: Schematic of energy and material flows (green: environmental energy, orange: energy conversion, blue: thermal storage, red: useful energy).

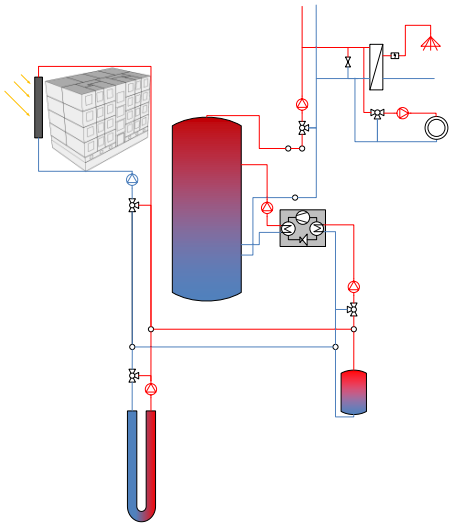

Fig. 8: Schematic diagram of the heat supply system under investigation

The operation of the solar façade as an additional heat source for the heat pump can significantly reduce the load on the borehole heat exchanger. Furthermore, regeneration mitigates short- and longtime temperature reduction of the ground and enables a sustainable operation of the system. As a result, a smaller BHE field, e.g. lower depth, less numbers or reduced spacing of the probes is possible. In this simulation, the reduction is about 25 %. Higher reductions up to 50% can be achieved depending on the operating conditions. The lower the set temperature the higher the performance of the façade but also the risks resulting from surface condensation and freezing as well as the impact on aesthetics and acceptance.

In this simulation, the min. allowed inlet temperature in the façade elements is set to -1 °C. The façade is operated as a heat source for the heat pump if the façade outlet temperature reaches temperatures above 8 K over evaporator outlet. This operation mode stops, if the temperature difference drops below 4 K. This mode is prioritized, to reduce the load of the borehole heat exchangers. In a second operation mode the façade is used to regenerate the ground and thus to enable a smaller dimensioning of the field. Regeneration takes place if the façade outlet temperature is at least 5 K over the outlet and stops as soon as the difference drops below 3 K.

The façade is modelled with the TRNSYS Type 832 (Haller et al., 2013), main collector parameters are shown in Tab. 5 and gained and validated from experimental measurements. The model was validated with measured values. Deviating from Tab. 3, the metal façade has different parameters, since not all measured values were available at the beginning of the simulation.

Tab. 5: Collector parameters of Type 832 for the selected façades

Symbol	**η_0**	**a_1**	**a_2**	**c_{whl}**	**c_{IR}**	**C_{eff}**	**c_{wf}**
Quantity	zero loss efficiency	Linear heat loss coefficient	Quadratic heat loss coefficient	Wind speed dependency of heat losses	Infrared radiation dependency of collector	Effective heat capacity	Wind speed dependency of the zero loss efficiency
Unit	-	W m^{-2} K^{-1}	W m^{-2} K^{-2}	J m^{-3} K^{-1}	-	J m^{-2} K^{-1}	s m^{-1}
Concrete	0.400	11.3028	-	4.04	-0.2125	282000	0.05192
Glass	0.774	9.3300	-	3.74	0	11000	0.029
Metal	0.602	11.3600	-	0.71	-0.628	14000	0.024
Glazed collector	0.775	5.11	0.0140	0	0	11000	0.14

In Fig. 9, the impact of different façade claddings are shown. For this 48 m² south, 33 m² east and 13 m² west façade are thermally activated.

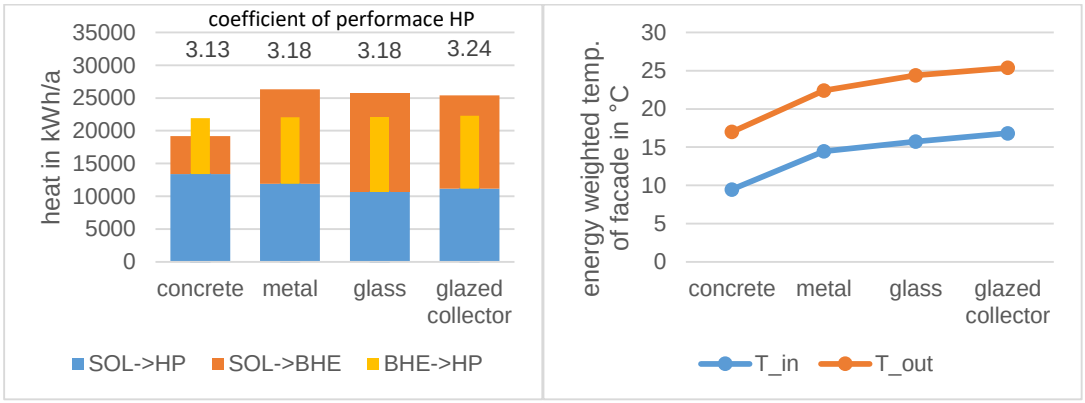

Fig. 9: Simulation results, left: heat flow of façade to geothermal probe for regeneration (SOL->BHE), façade as heat source for heat pump (SOL->HP) and geothermal probe as source for heat pump (BHE->HP); right: energy weighted inlet and outlet temperature of façade

Façades with higher efficiency could reach higher yields. Therefore in the simulation shown in Fig. 9 the use of the façade as a heat pump source is prioritized. At the same time higher temperature of the façade has to be usable to achieve higher system performance. In the investigated configuration the evaporator of heat pump as well as the inlet temperature of geothermal probes represent a limitation for the operating range of the active facade. In further work the potential of using heat from the façade to directly load the buffer storage has to be analyzed.

Simulation results with the concrete façade for different orientation and area are shown in Fig. 10.

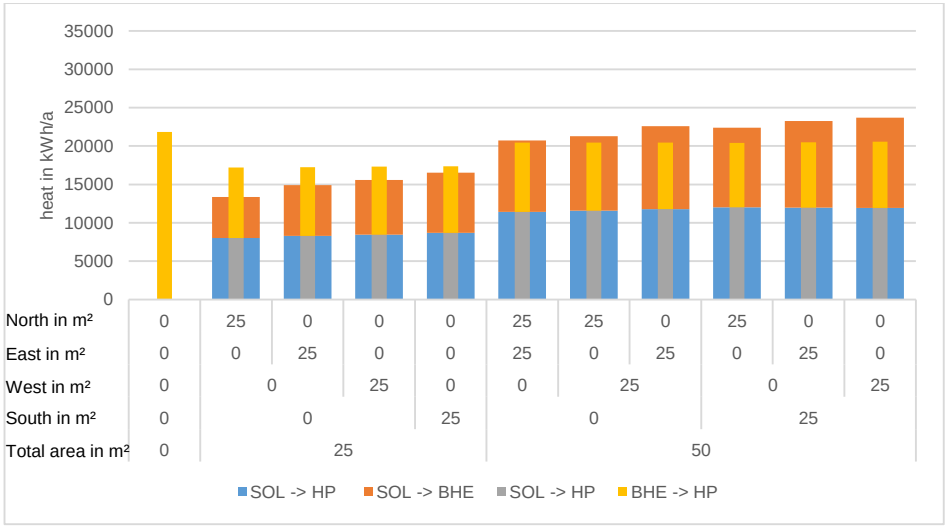

Fig. 10: Impact of area and orientation of concrete façade

The façade is used both as an environmental heat exchanger and as solar absorber, the highest yields are achieved on the south side, followed by west and east. A façade area of 25 m², e.g. south, supplies nearly 50% of total energy demand of the heat pump and actively regenerate the geothermal probes to 90 %.

6. Acknowledgments

The work is based on the results of the project "Solar-VHF", funded by the Lower Saxony Ministry of Science and Culture and by the German Federal Ministry of Economy and Energy (BMWi, reference number 03ETW013A-I), following a decision of the German Parliament. The investigations are carried out in cooperation with the Fraunhofer-Institut für Bauphysik and the German companies Konvortec GmbH & Co. KG, Systea Pohl

GmbH, Gundlach GmbH & Co. KG Wohnungsunternehmen, , Pforzheimer Bau und Grund GmbH and Clina Heiz- und Kühlelemente GmbH. The authors are grateful for the support and responsible for the content of the publication.

7. References

BBSR (2017) Ortsgenaue Testreferenzjahre (TRY) von Deutschland für mittlere und extreme Witterungsverhältnisse [Online]. Available at https://www.bbsr.bund.de/BBSR/DE/forschung/programme/zb/Auftragsforschung/5EnergieKlimaBauen/2013/testreferenzjahre/01-start.html (Accessed 5 October 2021).

Braas, H., Jordan, U., Best, I., Orozaliev, J. and Vajen, K., 2020. District heating load profiles for domestic hot water preparation with realistic simultaneity using DHWcalc and TRNSYS, Energy, vol. 201, p. 117552 [Online]. DOI: 10.1016/j.energy.2020.117552.

DIN, 18516-1:2010-06, 2010. Außenwandbekleidungen, hinterlüftet_- Teil_1: Anforderungen, Prüfgrundsätze, Beuth Verlag GmbH [Online]. DOI: 10.31030/1633660 (Accessed 7 October 2021).

DIN EN, 9806:2018-04, 2018. Solarenergie_- Thermische Sonnenkollektoren_- Prüfverfahren (ISO_9806:2017); Deutsche Fassung EN_ISO_9806:2017, Beuth Verlag GmbH [Online]. DOI: 10.31030/2681379 (Accessed 7 October 2021).

Frank, E., Haller, M., Herkel, S. and Ruschenburg, J., 2010. Systematic Classification of combined solar thermal and heat pump systems, Proceedings of the EuroSun 2010 Conference, Graz, Österreich, IEA-SHC.

FVHF, 2018. FVHF Guideline: Planning and Constructing Rear-Ventilated Rainscreen Facades, Fachverband Baustoffe und Bauteile für vorgehängte hinterlüftete Fassaden e.V. (FVHF) [Online]. Available at https://www.fvhf.de/Fassade-bilder/docs/FVHF-Guideline_Planning-and-Constructing-Rear-Ventilated-Rainscreen-Fac-ades_180306_EN.pdf (Accessed 27 August 2021).

Haller, M., Perers, B., Bales, C., Paavilainen, J., Dalibard, A., Fischer, S. and Bertram, E., 2013. TRNSYS Type 832 v5.01 „Dynamic Collector Model by Bengt Perers“: Updated Input-Output Reference, Report.

Jonas, D., 2019. Visualization of energy flows in PVT systems, IEA SHC Task 62 [Online]. DOI: 10.18777/ieashc-task60-2019-0001 (Accessed 25 February 2021).

Kirchner, M., Geissler, J., Hüsing, F. and Giovannetti, F., 2017. Solaraktivierte, hinterlüftete Glasfassade: Experimentelle Untersuchungen und Systemsimulationen, Bad Staffelstein.

Klein, S. A., 2014. TRNSYS 17 - A Transient Simulation Program, Solar Energy Laboratory, University of Wisconsin, Madison.

Mayer, E., Zegowitz, A. and Kersken, M., 2018. Messung des konvektiven Wärmeübergangs - Entwicklung eines neuen Sensors und bauphysikalische Anwendungen, Bauphysik, vol. 40, no. 5, pp. 336–343 [Online]. DOI: 10.1002/bapi.201800015.

S. Holst, 2010. Type 362 Dynamic radiator model with pipes (Type 162), Bayerisches Zentrum für angewandte Energieforschung e.V. [Online]. Available at https://trnsys.de/static/641c965bac4f593c3b4cc569839a51c2/Type_361_362_320_en.pdf.

SolMetall, 2017. Thermal conduction WLT, [Online]. Available at https://www.solmetall.de/en/absorber.php (Accessed 27 August 2021).